

A boundary integral approach to linear and nonlinear transient wave scattering

Aihua Lin, Anastasiia Kuzmina and Per Kristen Jakobsen

Department of Mathematics and Statistics, UIT the Arctic
University of Norway, 9019 Tromsø, Norway

Abstract

In this work, we introduce a method for solving linear and nonlinear scattering problems for wave equations using a new hybrid approach. This new approach consists of a reformulation of the governing equations into a form that can be solved by a combination of a domain-based method and a boundary-integral method. Our reformulation is aimed at a situation in which we have a collection of compact scattering objects located in an otherwise homogeneous unbounded space.

The domain-based method is used to propagate the equations governing the wave field inside the scattering objects forward in time. The boundary integral method is used to supply the domain-based method with the required boundary values for the wave field.

In this way, the best features of both methods come into play. The response inside the scattering objects, which can be caused by both material inhomogeneity and nonlinearities, is easily considered using the domain-based method, and the boundary conditions supplied by the boundary integral method makes it possible to confine the domain-method to the inside of each scattering object.

1 Introduction

Boundary integral formulations are well known in all areas of science and technology and lead to highly efficient numerical algorithms for solving partial differential equations (PDEs). Particularly, their utility is evident for scattering waves from objects located in an unbounded space. For these situations, one whole space dimension is taken out of the problem by reducing the solution of the original PDEs to the solution of an integral equation located on the boundaries of the scattering objects.

However, this reduction relies on the use of Green's functions and is therefore only possible if the PDEs are linear. For computational reasons, one is also usually restricted to situations in which Green's functions are given by explicit formulas, which rules out most situations in which the materials are inhomogeneous. Since many problems of interest involve scattering waves from objects that display both material inhomogeneity and nonlinearity, boundary integral methods have appeared to be of limited utility in computational science. Adding to the limited scope of the method, the fact that somewhat advanced

mathematical machinery is needed to formulate PDEs in terms of boundary integral equations, it is perhaps not difficult to understand why the method is that popular.

Domain-based methods, like the finite difference method and finite element method, appear to have much wider utility. Their simple formulation and wide applicability to many types of PDEs, both linear and nonlinear, have made them extremely popular in the scientific computing community. In the context of scattering problems, they have problems of their own to contend with. These problems are of two quite distinct types.

The first type of problem is related to the fact that the scattering objects frequently represent abrupt changes in material properties compared to the properties of the surrounding homogeneous space. This abrupt change leads to PDEs with discontinuous or near-discontinuous coefficients. Such features are hard to represent accurately using the finite element or finite difference methods. The favored approach is to introduce multiple, interlinked grids that are adjusted so that they conform to the boundaries of the scattering objects. Generating such grids, tailored to the possibly complex shape of the scattering objects, linking them together in the correct way and designing them in such a way that the resulting numerical algorithm is accurate and stable, is challenging. The approach has been refined over many years and in general works quite well, but it certainly adds to the implementation complexity of these methods.

The second type of problem is related to the fact that one cannot grid the domain where the scattering objects are located for the simple reason, that in almost all situations of interest, this domain is unbounded. This problem is well known in the research community and the way it is resolved is to grid a computational box that is large enough to contain all scattering objects of interest. This can easily become a very large domain, leading to a very large number of degrees of freedom in the numerical algorithm. However, most of the time, the numerical algorithm associated with the domain has a simple structure for which it is possible to design very fast implementations. However, the introduction of the finite computational box in what is an unbounded domain leads to the question of designing boundary conditions on the boundary of the box so that it is fully transparent to waves. This is not easy to achieve, as most approaches will introduce inhomogeneity that will partly reflect the waves hitting the boundary. This problem was first solved satisfactorily for the case of scattering electromagnetic waves. The domain-based method of choice for electromagnetic waves is the finite difference time domain method (FDTD) [1],[2],[3]. As the name indicates, this is a finite difference method that has been designed to consider the special structure of Maxwell's equations. The removal of reflections from the finite computational box was achieved by the introduction of a perfectly matched layer (PML)[4],[5]. This amounts to adding a narrow layer of a specially constructed artificial material to the outside of the computational box. The PML layer is only perfectly transparent to wave propagation if the grid has infinite resolution. For any finite grid there is still a small reflection from the boundary of the computational box. This can be reduced by making the PML layer thicker, but this leads to more degrees of freedom and thus an increasing computational load. However, overall PML works well and certainly much better than anything that came before it. There is no doubt that the introduction of PML was a breakthrough.

The use of PML was closely linked to the special structure of Maxwell's

equations. However, it was soon realized that the same effect could be achieved by complexifying the physical space outside the computational box and analytically continuing the fields into this complex spatial domain[6],[7]. Significantly, this realization made the benefits of a reflection-less boundary condition available to all kinds of scattering problems. However, the use of these reflection less boundary conditions certainly leads to an increased computational load, increased implementation complexity, and numerical stability issues that must be resolved. It is at this point worth recalling that the boundary of the computational box is not part of the original physical problem, and all the added implementation complexity and computational cost is spent trying to make it invisible after the choice of a domain method forced us to put it there in the first place.

In this paper, we are dedicated to developing an efficient new method to solve transient wave scattering in two 1D models in which the scattering objects have a nonlinear response where we only apply the domain-based method inside each scattering object. First, this will reduce the size of the computational grid enormously since we now need only to grid the inside of the scattering objects. Second, our approach makes it possible to use different computational grids for each scattering object, with each grid tailored to the corresponding object's geometric shape, without having to worry about the inherent complexity caused by letting the different grids meet up. Third, it makes the introduction of a large computational box, with its artificial boundary, redundant. In this way, the computational load is substantially reduced, and we remove the implementation complexity and instabilities associated with the boundary of the computational box.

However, the domain based-method restricted to the inside of each scattering object requires field values on the boundaries of the scattering objects to propagate the fields forward in time. These boundary values will be supplied by a boundary integral method derived from a space-time integral formulation of the PDEs to be solved. This boundary integral method will consider all the scattering and re-scattering of the solution to the PDEs in the unbounded domain outside the scattering objects. Since the boundary integral method explicitly considers the radiation condition at infinity, no finite computational box with its artificial boundary conditions is needed.

This kind of idea for solving scattering problems was, to our knowledge, first proposed in 1972 by Pattanayak and Wolf [8] for the case of electromagnetic waves. They discussed their ideas in the context of a generalization of the Ewald-Oseen optical extinction theorem; therefore, we will refer to our method as the Ewald-Oseen Scattering(EOS) formulation.

However, Pattanayak and Wolf only discussed stationary linear scattering of electromagnetic waves and they therefore did their integral formulation in frequency space. This approach is not the right one when one is interested in transient scattering from objects that are generally inhomogeneous and additionally may have a nonlinear response. What is needed for our approach is a space-time integral formulation of the PDEs of interest.

In sections 2 and 3, we illustrate our approach by implementing our EOS formulation for two different 1D scattering problems. Both cases can be thought of as toy models for scattering electromagnetic waves. This should not be taken to mean that only models that in some way are related to electromagnetic scattering can be subject to our approach. It merely reflects our particular interest

in electromagnetic scattering. The way we see it, only one essential requirement must be fulfilled for our method to be applicable. It must be possible to derive an explicit integral formulation for the PDEs of interest. This means that at some point one needs to find the explicit expression for Green's function for some differential operator related to our PDEs. In general, it is difficult to find explicit expressions for Green's function belonging to nontrivial differential operators. However, the Green's function needed for our EOS formulation will always be of the infinite, homogeneous space type, and explicit expressions for such Green's functions can frequently be found.

The two toy models presented in this work have been chosen for their simplicity, which makes them well suited for illustrating our EOS approach for scattering of waves. For more general and consequently more complicated cases, there are no new ideas beyond the technical details that must be mastered for each case to derive the EOS formulation and implement it numerically. To explore the feasibility of our approach for more realistic and useful PDEs, we have implemented our approach for several other cases, both 2D and 3D. Particularly we have derived and implemented our EOS approach for the full 3D vector Maxwell's equations. The results of these investigations will be reported elsewhere.

For both models we use an approach for testing the stability and accuracy of our implementations that involves what is known as *artificial sources*. This method has probably been around for a long time but apart from an application to the Navier-Stokes equations [9], we are not aware of any published work using this method. The method is based on the simple observation that, if arbitrary source terms are added to any system of PDEs then any function is a solution for some choice of the source. Adding a source term typically introduce only trivial modifications to whichever numerical method was used to solve the PDEs. This essentially means that for any PDEs of interest, we can design particular functions to test various critical aspects of the numerical method related to numerical stability and accuracy.

This is a very simple approach to validating numerical implementations for PDEs that deserves to be much better known than it is.

2 The first scattering model; one way propagation

Our first toy model, model 1, is

$$\begin{aligned}\varphi_t &= c_1 \varphi_x + j, \\ \rho_t &= -j_x, \\ j_t &= (\alpha - \beta \rho) \varphi - \gamma j \quad a_0 < x < a_1,\end{aligned}\tag{2.1}$$

where α, β and γ are real parameters determining the “material response” part model 1 and where $\varphi = \varphi(x, t)$ is the “electric field”, $j = j(x, t)$ the “current density” and ρ the “charge density”. These quantities are analogs for the corresponding quantities in Maxwell's equations. With this in mind, we observe that the second equation in the model (2.1) is a 1D version of the equation of continuity from electromagnetics, and c_1 is the analog of the speed of light inside

the “material” scattering object residing inside the interval $[a_0, a_1]$. The charge density and current density are the material degrees of freedom and are therefore assumed to be confined to the interval $[a_0, a_1]$ on the real axis, whereas φ is a field defined on the whole real axis. Thus the interval $[a_0, a_1]$ is the analog of a compact scattering object in the electromagnetic situation. Outside the scattering object the model takes the form

$$\varphi_t = c_0 \varphi_x + j_s \quad x < a_0 \text{ or } x > a_1, \quad (2.2)$$

where c_0 is the propagation speed for the electric field in the “vacuum” outside the scattering object and the function $j_s(x, t)$ is a fixed source that has its support in a compact set in the interval $x > a_1$. For the field φ we impose the condition of continuity at the points a_0 and a_1 . The equation for the current density, j is a radical simplification of a real current density model used to describe second harmonic generation in nonlinear optics [10].

2.1 The EOS formulation

In order to derive the EOS formulation for the model (2.1), we will firstly need a space-time integral identity involving the operator

$$L = \partial_t - v \partial_x,$$

where v is some constant. Using integration by parts it is easy to see that the following integral identity holds

$$\begin{aligned} & \int_{S \times T} dx dt \{ L \varphi(x, t) \psi(x, t) - \varphi(x, t) L^\dagger \psi(x, t) \} \\ &= \int_S dx \varphi(x, t) \psi(x, t) \Big|_{t_0}^{t_1} - v \int_T dt \varphi(x, t) \psi(x, t) \Big|_{x_0}^{x_1}, \end{aligned} \quad (2.3)$$

where $L^\dagger = -\partial_t + v \partial_x$ is the formal adjoint of L and where $S = (x_0, x_1)$ and $T = (t_0, t_1)$ are open space and time intervals.

The second item we need in order to derive the EOS formulation for model (2.1), is the advanced Green's function for the operator L^\dagger . This is a function $G = G(x, t, x', t')$ which is a solution to the equation

$$L^\dagger G(x, t, x', t') = \delta(t - t') \delta(x - x'),$$

and that vanishes when $t > t'$. Since the operator \mathcal{L}^+ is invariant under time and space translations we can without loss of generality assume that

$$G(x, t, x', t') = G(x - x', t - t').$$

Thus it is sufficient to solve the equation

$$L^\dagger G(x, t) = \delta(x) \delta(t). \quad (2.4)$$

After performing the Fourier transform

$$\hat{f}(k, \omega) = \int_{-\infty}^{\infty} \int_{-\infty}^{\infty} f(x, t) e^{-i(kx - \omega t)} dx dt, \quad (2.5)$$

on (2.4), we get

$$\hat{G}(k, \omega) = \frac{-i}{\omega + vk}.$$

It is noticed that there's a single pole at $\omega = -vk$ on the real axis, we need to find the advanced Green's function. It is defined by shifting the integral contour from the real ω -axis to a contour below and parallel to the real axis at a distance $c_\epsilon : z = \omega - i\epsilon, \epsilon > 0$. Using the inverse Fourier transform

$$f(x, t) = \frac{1}{4\pi^2} \int_{-\infty}^{\infty} \int_{-\infty}^{\infty} \hat{f}(k, \omega) e^{i(kx - \omega t)} dk d\omega, \quad (2.6)$$

we get the representation

$$G(x, t) = \frac{1}{4\pi^2} \int_{-\infty}^{+\infty} g(k, t) e^{ikx} dk,$$

with

$$g(k, t) = \int_{c_\epsilon} \frac{-i}{z + vk} e^{-izt} dz.$$

For $t < 0$, we close the contour c_ϵ in the upper half plane and get by Cauchy's residue theorem

$$g(k, t) = 2\pi e^{ivkt},$$

and for $t > 0$, we close the contour c_ϵ in the lower half plane and get $g(k, t) = 0$. This gives for $t < 0$

$$G(x, t) = \frac{1}{4\pi^2} \int_{-\infty}^{+\infty} 2\pi e^{ivkt} e^{ikx} dk = \delta(x + vt),$$

and for $t > 0$,

$$G(x, t) = 0.$$

In the end G is given by

$$G(x, t, x', t') = \theta(t' - t) \delta(x' - x + v(t' - t)), \quad (2.7)$$

where θ is the Heaviside step function with $\theta(x) = 1$ for $x > 0$ and zero otherwise.

We will now apply the integral identity (2.3) to each space interval $(-\infty, a_0)$, (a_0, a_1) and (a_1, ∞) . For the function ψ we will substitute the advanced Green's function (2.7) and we will let φ be the solution to equation (2.2) with vanishing initial condition, $\varphi(x, t_0) = 0$. We thus have a problem where all solutions are purely source-generated. For the first interval, $(-\infty, a_0)$, we let ψ be the Green's function

$$G_0(x, t, x', t') \equiv \theta(t' - t) \delta(x' - x + c_0(t' - t)), \quad (2.8)$$

and $\varphi = \varphi_0$ be the solution to the equation

$$\begin{aligned} \varphi_{0t} &= c_0 \varphi_{0x}, \\ &\Updownarrow \\ L_0 \varphi_0 &= 0. \end{aligned} \quad (2.9)$$

Inserting (2.8), (2.9) and $S = (-\infty, a_0)$ into the integral identity (2.3), using the initial condition and the fact that the Green's function is advanced, we get for x in $(-\infty, a_0)$

$$\begin{aligned}
& \int_{S \times T} \{ \mathcal{L}\varphi_0(x', t') G(x', t', x, t) - \varphi_0(x', t') \mathcal{L}^+ G(x', t', x, t) \} dx' dt' \\
&= \int_{-\infty}^{a_0} \varphi_0(x', t_1) \theta(t - t_1) \delta(x - x' + c_0(t - t_1)) dx' \\
&- \int_{-\infty}^{a_0} \varphi_0(x', t_0) \theta(t - t_0) \delta(x - x' + c_0(t - t_0)) dx' \\
&- c_0 \int_{t_0}^{t_1} \varphi_0(a_0, t') \theta(t - t') \delta(x - a_0 + c_0(t - t')) dt' \\
&+ c_0 \lim_{x' \rightarrow -\infty} \int_{t_0}^{t_1} \varphi_0(x', t') \theta(t - t') \delta(x - x' + c_0(t - t')) dt',
\end{aligned}$$

after interchanging the primed and unprimed variables. The initial condition and $t_0 < t < t_1$ imply that the integrals on S vanish. The last integral vanishes also because $x - x' + c_0(t - t') > 0$ when $x' < x$ for all t' in the integration interval (t_0, t) . So we finally get

$$\varphi_0(x, t) = c_0 \int_{t_0}^t dt' \varphi_0(a_0, t') \delta(x - a_0 + c_0(t - t')). \quad (2.10)$$

Note that when writing formula (2.10) we have made the substitution

$$\varphi_0(a_0, \cdot) \equiv \lim_{x \rightarrow a_0^-} \varphi_0(x, \cdot).$$

Similar substitutions will be made without comment later in the following sections.

For the second interval, (a_0, a_1) , we let ψ be the Green's function

$$G_1(x, t, x', t') \equiv \theta(t' - t) \delta(x' - x + c_1(t' - t)), \quad (2.11)$$

and $\varphi = \varphi_1$ be the solution to the equation

$$\begin{aligned}
\varphi_{1t} &= c_1 \varphi_{1x} + j, \\
&\Downarrow \\
L_1 \varphi &= j,
\end{aligned} \quad (2.12)$$

with vanishing initial conditions. Inserting (2.11), (2.12) and $S = (a_0, a_1)$ into the integral identity (2.3), using the initial condition and the fact that the

Green's function is advanced, we get for x in (a_0, a_1)

$$\begin{aligned}
\varphi_1(x, t) &= \int_{a_0}^{a_1} dx' \int_{t_0}^t dt' j(x', t') \delta(x - x' + c_1(t - t')) \\
&\quad + c_1 \int_{t_0}^t dt' \varphi_1(a_1, t') \delta(x - a_1 + c_1(t - t')) \\
&\quad - c_1 \int_{t_0}^t dt' \varphi_1(a_0, t') \delta(x - a_0 + c_1(t - t')) \\
&= \int_{a_0}^{a_1} dx' \int_{t_0}^t dt' j(x', t') \delta(x - x' + c_1(t - t')) \\
&\quad + c_1 \int_{t_0}^t dt' \varphi_1(a_1, t') \delta(x - a_1 + c_1(t - t')), \tag{2.13}
\end{aligned}$$

after interchanging primed and unprimed variables. The last equality sign follows because $x - a_0 + c_1(t - t') > 0$ for all t' in the integration interval when $a_0 < x < a_1$.

Finally, for the third integration interval, (a_1, ∞) , we let ψ be the Green's function

$$G_0(x, t, x', t') \equiv \theta(t' - t) \delta(x' - x + c_0(t' - t)), \tag{2.14}$$

and $\varphi = \varphi_2$ be the solution to the equation

$$\begin{aligned}
\varphi_{2t} &= c_0 \varphi_{2x} + j_s, \\
&\quad \Downarrow \\
L_0 \varphi_2 &= j_s, \tag{2.15}
\end{aligned}$$

with vanishing initial conditions. Inserting (2.14), (2.15) and $S = (a_1, \infty)$ into the integral identity (2.3), using the initial conditions and the fact that the Green's function is advanced, we get for x in (a_1, ∞)

$$\begin{aligned}
\varphi_2(x, t) &= \int_{a_1}^{\infty} dx' \int_{t_0}^t dt' j_s(x', t') \delta(x - x' + c_0(t - t')) \\
&\quad + c_0 \lim_{x' \rightarrow \infty} \int_{t_0}^t dt' \varphi_2(x', t') \delta(x - x' + c_0(t - t')) \\
&\quad - c_0 \int_{t_0}^t dt' \varphi_2(a_1, t') \delta(x - a_1 + c_0(t - t')) \\
&= \int_{a_1}^{\infty} dx' \int_{t_0}^t dt' j_s(x', t') \delta(x - x' + c_0(t - t')), \tag{2.16}
\end{aligned}$$

after interchanging primed and unprimed variables. The third term vanishes because $x - a_1 + c_0(t - t') > 0$ for all t' in the integration interval when $x > a_1$. The second term vanishes because $x - x' + c_0(t - t') < 0$ for all fixed $x > a_1$, $t > t_0$ and all t' in the integration interval (t_0, t) when x' is large enough.

We now investigate the limit of these integral identities as x approaches the boundary points $\{a_0, a_1\}$ of the open interval (a_0, a_1) from inside and outside the interval. This will give us four equations for the four quantities

$$\varphi(a_0, t), \varphi_1(a_0, t), \varphi_1(a_1, t), \varphi_2(a_1, t).$$

However, by assumption, acceptable solutions of model 1 are continuous across the boundary points $\{a_0, a_1\}$. Therefore, we have two additional equations

$$\begin{aligned}\varphi_0(a_0, t) &= \varphi_1(a_0, t), \\ \varphi_1(a_1, t) &= \varphi_2(a_1, t).\end{aligned}$$

At this point we are faced with a problem. The four unknown quantities must satisfy six linear equations. The problem is thus overdetermined and we would not normally expect any nontrivial solutions to exist.

On the other hand, the equations, boundary conditions and source function j_s that define model 1 do determine a unique function φ . This function satisfies by construction the integral identities (2.10), (2.13) and (2.16), whose limits yielded the overdetermined system. Thus the overdetermined linear system does have a solution.

There is a more direct way to see why the overdetermined system will have a solution. Let us consider the inside of the scattering object, thus $x \in (a_0, a_1)$. Here, the field φ is determined in terms of the current $j(x, t)$, and the boundary value $\varphi(a_1, t)$ by identity (2.13)

$$\begin{aligned}\varphi_1(x, t) &= \int_{a_0}^{a_1} dx' \int_{t_0}^t dt' j(x', t') \delta(x - x' + c_1(t - t')) \\ &\quad + c_1 \int_{t_0}^t dt' \varphi_1(a_1, t') \delta(x - a_1 + c_1(t - t')).\end{aligned}\quad (2.17)$$

Naively, one would expect that we would obtain an equation determining the unknown boundary value $\varphi(a_1, t)$, by taking the limit of (2.17) as x approaches a_1 from below. However, this would make the field inside the scattering object independent of the outside source, which must be wrong from a scattering point of view. After all, it is the outside source $j_s(x, t)$ that determines the field both outside and inside the scattering object. If this source is turned off the field would simply be zero everywhere. So what is going on?

Note that if we actually take the limit of (2.17) we get the equation

$$0 \varphi_1(a_1, t) = 0,$$

which leaves the boundary value entirely arbitrary. If we analyze the rest of the overdetermined system in the same way, we find that one more equation for the boundary data is redundant, and that the two unknown boundary values, $\varphi_1(a_0, t)$ and $\varphi(a_1, t)$, are uniquely determined by the following two equations

$$\begin{aligned}\varphi_1(a_0, t) &= \int_{a_0}^{a_1} dx' \theta(a_0 - x' + c_1(t - t_0)) j(x', t - \frac{a_1 - a_0}{c_1}) \\ &\quad + \theta(a_0 - a_1 + c_1(t - t_0)) \varphi(a_1, t - \frac{a_1 - a_0}{c_1}),\end{aligned}\quad (2.18)$$

$$\varphi_1(a_1, t) = \frac{1}{c_0} \int_{a_1}^{\infty} dx' \theta(a_1 - x' + c_0(t - t_0)) j_s(x', t - \frac{x' - a_1}{c_0}).\quad (2.19)$$

We emphasize the fact that we end up with an overdetermined system of linear equations for the boundary values because this is a generic outcome when we derive the EOS formulation for any given system of PDEs. We see that this

very same problem will appear when we discuss the second toy model in Section 3.

This problem has been recognized by the research community in the context of space-time boundary integral formulation for Maxwell's equations, and a simple fix has been invented to resolve it.

However, as far as we know, the universal nature of this problem in the area of space-time integral formulations of linear and nonlinear scattering problems has not been recognized.

Observe that equation (2.19) determines the value of the field at the boundary point a_1 in terms of the given external source j_s , and the equation (2.18) determines the value of the field at the boundary point a_0 in terms of the current density j inside the scattering object and the field values at the boundary point a_1 .

Equations (2.1) restricted to the the open interval (a_0, a_1) together with the integral identities (2.18) and (2.19) define the EOS formulation for model 1.

2.2 Numerical implementation of the EOS formulation

In this section, a numerical implementation of the EOS formulation for model 1 is presented. Many different numerical implementations are possible. The EOS formulation itself does not in any way dictate the use of a particular implementation. However it does put some constraints on how we proceed with our method of choice.

If our problem was to calculate the free-space propagation according to the first equation in (2.1) with vanishing j the obvious choice would be to use the standard Lax-Wendroff method[11] on a uniform space grid. However, the EOS formulation presents us with an integro-differential equation because the boundary update rule is defined in terms of integrals of the current density over the scattering domain (a_0, a_1) . Thus our grid must also give a good approximation for the integrals (2.18) and (2.19) that define the update rule. We will be looking for second-order accuracy and would like to use the midpoint rule to approximate the integrals and thus introduce the following nonuniform space grid inside the scattering object, (a_0, a_1) ,

$$x_i = a_0 + (i + 0.5)\Delta x, \quad i = 0, 1, \dots, N - 1, \quad (2.20)$$

where $\Delta x = \frac{a_1 - a_0}{N}$. The grid points (2.20) will be called internal nodes. We also introduce a discrete time grid

$$t^n = n\Delta t, \quad n = 0, 1, \dots$$

The values of the parameter Δt will, as usual, be bounded by the requirement of stability for the scheme. We will say a few words about this bound later.

To obtain a numerical scheme of second-order accuracy, we apply the Lax-Wendroff method to the first two equations of (2.1) and apply the modified Euler's method to the last equation of (2.1). Because of these choices the nu-

merical scheme for iteration at the internal nodes takes the form

$$\begin{aligned}
\varphi_i^{n+1} &= \varphi_i^n + \Delta t (c_1 \frac{\partial \varphi}{\partial x} + j)_i^n + \frac{1}{2} (\Delta t)^2 (c_1^2 \frac{\partial^2 \varphi}{\partial x^2} + c_1 \frac{\partial j}{\partial x} + f)_i^n, \\
\rho_i^{n+1} &= \rho_i^n + \Delta t (-\frac{\partial j}{\partial x})_i^n + \frac{1}{2} (\Delta t)^2 (-\frac{\partial f}{\partial x})_i^n, \\
\bar{j}_i^{n+1} &= j_i^n + \Delta t f_i^n, \\
j_i^{n+1} &= \frac{1}{2} (j_i^n + \bar{j}_i^{n+1} + \Delta t f(\rho_i^{n+1}, \varphi_i^{n+1}, \bar{j}_i^{n+1})),
\end{aligned} \tag{2.21}$$

for $i = 0, 1, \dots, N$ and where $f = (\alpha - \beta\rho)\varphi - \gamma j$. Except for the two internal nodes closest to the boundary points a_0 and a_1 , the space derivatives are approximated to second-order accuracy by the following standard finite difference formulas

$$\begin{aligned}
(\frac{\partial \phi}{\partial x})_i^n &= \frac{\phi_{i+1}^n - \phi_{i-1}^n}{2\Delta x}, \\
(\frac{\partial^2 \phi}{\partial x^2})_i^n &= \frac{\phi_{i+1}^n - 2\phi_i^n + \phi_{i-1}^n}{(\Delta x)^2}, \quad \phi = \varphi, j, f, \text{ and } i = 1, 2, \dots, N-2.
\end{aligned} \tag{2.22}$$

For the two internal nodes closest to the boundary, the standard, second-order accurate difference formulas, cannot be used because the internal nodes are non-uniformly distributed in this part of the domain. For the field, φ , we must rather use the following second-order accurate difference formulas for these two nodes

$$\begin{aligned}
(\frac{\partial \varphi}{\partial x})_0^n &= -\frac{1}{3\Delta x} (4\varphi_{a_0}^n - 3\varphi_0^n - \varphi_1^n), \\
(\frac{\partial^2 \varphi}{\partial x^2})_0^n &= \frac{4}{3(\Delta x)^2} (2\varphi_{a_0}^n - 3\varphi_0^n + \varphi_1^n), \\
(\frac{\partial \varphi}{\partial x})_{N-1}^n &= \frac{1}{3\Delta x} (4\varphi_{a_1}^n - 3\varphi_{N-1}^n - \varphi_{N-2}^n), \\
(\frac{\partial^2 \varphi}{\partial x^2})_{N-1}^n &= \frac{4}{3(\Delta x)^2} (2\varphi_{a_1}^n - 3\varphi_{N-1}^n + \varphi_{N-2}^n).
\end{aligned} \tag{2.23}$$

The boundary value $\varphi_{a_0}^n$ needed in formulas (2.23) can be calculated from the discretized form of the integral update rules (2.18)

$$\begin{aligned}
\varphi_{a_0}^{n+1} &= \frac{\Delta x}{c_1} \sum_{i=0}^{N-1} \theta(t_{n+1} - t_0 - \frac{x_i - a_0}{c_1}) j(x_i, t_{n+1} - \frac{x_i - a_0}{c_1}), \\
&+ \theta(t_{n+1} - t_0 - \frac{a_1 - a_0}{c_1}) \varphi(a_1, t_{n+1} - \frac{a_1 - a_0}{c_1}),
\end{aligned} \tag{2.24}$$

while $\varphi_{a_1}^n$ is determined by the outside source using (2.19).

The current density, j , is entirely supported inside the scattering object and in general would be discontinuous at a_0 and a_1 if extended to the whole domain by making it zero external to the scattering object. Because of this, we need difference rules for j at the nodes closest to the boundary points a_0 and a_1 that only depend on the values of j on internal nodes. The following second-order

accurate difference rules for j are of this type

$$\begin{aligned} \left(\frac{\partial j}{\partial x}\right)_0^n &= \frac{1}{2\Delta x}(4j_1^n - 3j_0^n - j_2^n), \\ \left(\frac{\partial j}{\partial x}\right)_{N-1}^n &= -\frac{1}{2\Delta x}(4j_{N-2}^n - 3j_{N-1}^n - j_{N-3}^n). \end{aligned} \quad (2.25)$$

It is evident that the discretized boundary update rule (2.24) needs values of the current density that are located between the grid points for the time grid $\{t^n\}$. This situation is general and will always arise when we seek numerical implementations of EOS formulations of PDEs. Some numerical interpolation scheme will always be needed to calculate the field values and/or the material variables between the time grid locations. We use a quadratic interpolation for values of the current density located between two time levels to maintain overall second-order accuracy for our scheme.

The iteration (2.21) with the boundary update rule (2.24) supplemented by the finite difference rules (2.22),(2.23) and (2.25) constitute our numerical implementation of the EOS formulation for model 1.

2.3 Artificial source test

The basic idea behind the artificial source test, of some numerical scheme designed for a system of PDEs, is to slightly modify the system by adding an arbitrary source to all the equations in the system. This modification typically leads to minimal modifications to the numerical scheme, where most of the effort and complexity are usually spent on the derivatives and nonlinear terms. For the equations, however, the presence of the sources changes the situation completely. This is because the presence of the added sources implies that *any* function is a solution to the equations for *some* choice of sources.

With the risk of expanding on perhaps an already obvious idea, what we are saying is that, if we have developed a numerical scheme for some system of differential equations $\mathcal{L}\psi = 0$, we can with small modifications extend our scheme to the extended equation $\mathcal{L}\psi = g$ where g is any given function. Given this, we test the numerical scheme by picking a function ψ_0 , then use the equation to calculate the source function $g_0 = \mathcal{L}\psi_0$ that ensures that our chosen function is a solution to the extended equation. Finally, we run the numerical scheme with the calculated source function and find an approximate solution that we compare with the exact solution ψ_0 .

Mode 1 extended with artificial sources takes the form

$$\begin{aligned} \varphi_t &= c_1\varphi_x + j + g_1, \\ \rho_t &= -j_x + g_2, \\ j_t &= (\alpha - \beta\rho)\varphi - \gamma j + g_3, \end{aligned} \quad (2.26)$$

where g_1, g_2, g_3 , are the artificial source functions. For some choice of functions $\hat{\varphi}, \hat{j}$ and $\hat{\rho}$ the corresponding source functions are computed by

$$\begin{aligned} \hat{g}_1 &= \hat{\varphi}_t - c_1\hat{\varphi}_x - \hat{j}, \\ \hat{g}_2 &= \hat{\rho}_t + \hat{j}_x, \\ \hat{g}_3 &= \hat{j}_t - (\alpha - \beta\hat{\rho})\hat{\varphi} + \gamma\hat{j}. \end{aligned}$$

As our exact solution we choose

$$\begin{aligned}\hat{\varphi}(x, t) &= \frac{2A_1}{\pi} \arctan(b^2 t^2) e^{-\alpha_1(x-x_o+\beta_1(t-t_s))^2}, \\ \hat{j}(x, t) &= A_2 e^{-\frac{(x-x_j)^2}{\delta_1^2} - \frac{(t-t_j)^2}{\delta_2^2}}, \\ \hat{\rho}(x, t) &= A_3 e^{-\frac{(x-x_\rho)^2}{\delta_3^2} - \frac{(t-t_\rho)^2}{\delta_4^2}},\end{aligned}\tag{2.27}$$

which is nowhere near a solution to the equations (2.2) defining the unmodified model 1. Note that the chosen exact solution satisfies the vanishing of the initial data $\hat{\varphi}(x, t_0) = 0$, as it must in order to be consistent with the EOS formulation. The boundary update rule for the source extended model (2.26) is changed into

$$\begin{aligned}\varphi_{a_0}^{n+1} &= \frac{\Delta x}{c_1} \sum_{i=0}^{N-1} \theta(t_{n+1} - t_0 - \frac{x_i - a_0}{c_1}) j(x_i, t_{n+1} - \frac{x_i - a_0}{c_1}), \\ &+ \frac{\Delta x}{c_1} \sum_{i=0}^{N-1} \theta(t_{n+1} - t_0 - \frac{x_i - a_0}{c_1}) \hat{j}_1(x_i, t_{n+1} - \frac{x_i - a_0}{c_1}), \\ &+ \theta(t_{n+1} - t_0 - \frac{a_1 - a_0}{c_1}) \hat{\varphi}(a_1, t_{n+1} - \frac{a_1 - a_0}{c_1}),\end{aligned}$$

while $\hat{\varphi}_{a_1}^n$ is given explicitly by the exact solution $\hat{\varphi}(x, t)$. The comparison

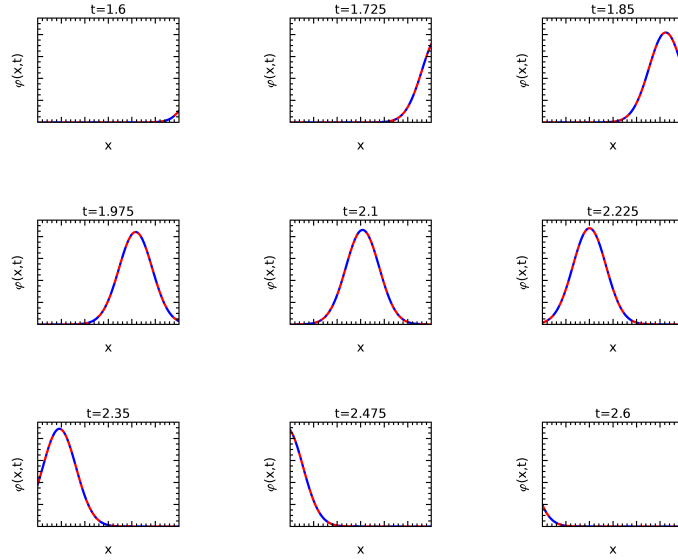


Figure 2.1: Comparison between the numerical solution and the exact solution for the source extended model 1. Parameter values used are $a_0 = 0.0, a_1 = 3.0, N = 1600, \alpha = -1.0, \beta = 0.3, \gamma = 8.0, c = 2.0, c_0 = 1.0, A_1 = 1.0, A_2 = 1.0, A_3 = 1.0, b = 1.0, \alpha_1 = 4.0, \beta_1 = 4.0, x_o = 6.0, t_s = 1.0, x_j = 1.1, x_\rho = 1.3, t_j = 1.2, t_\rho = 1.3, \delta_1 = 0.3, \delta_2 = 0.32, \delta_3 = 1.0, \delta_4 = 0.33$.

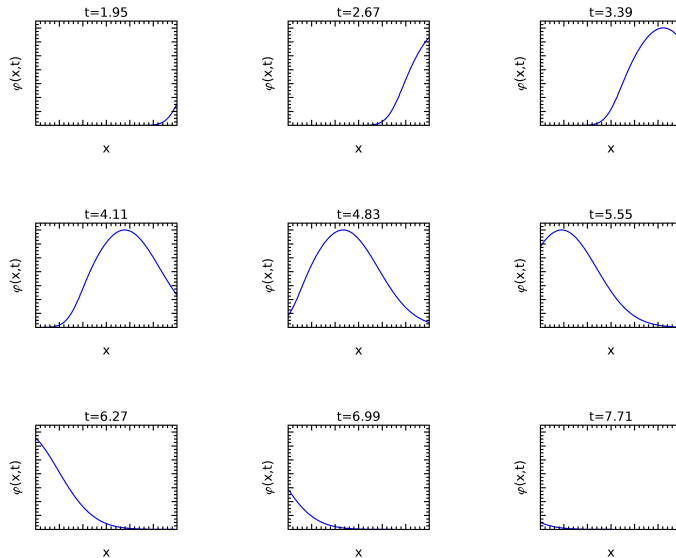


Figure 2.2: A numerical solution of the EOS formulation for model 1 generated by an external source. The parameter values used are $a_0 = 0.0$, $a_1 = 3.0$, $N = 1600$, $c = 2.0$, $c_0 = 1.0$, $\alpha = -1.0$, $\beta = 0.3$, $\gamma = 8.0$.

between the exact solution (2.27) and the approximative solution generated by our numerical implementation of the EOS formulation of the source extended model 1, (2.26), is shown in Fig 2.1 for some choice of the parameters. As we can see, the correspondence between the exact and approximative solution is excellent. After having established that our implementation is accurate using the artificial source test, we show in Fig 2.2 the numerical solution φ of model 1, (2.1), where the system is driven by an outside source of the form

$$j_s = 5e^{-36(x-4)^2 - 4(t-0.5)^2},$$

which is chosen so that no influence hit the boundary at a_1 before $t = 0$. This will ensure that the initial condition $\varphi(x, t = 0) = 0$, underlying the EOS formulation of model 1, is satisfied.

In these simulations we used a Δt which is in the stable range for the numerical implementation, specifically we used $\Delta t = 0.4 \frac{\Delta x}{c}$. Observe that the stability domain for our implementation of the EOS formulation is restricted compared to the stability domain for the underlying Lax-Wendroff method on an infinite domain. The focus of the first two sections is to derive the EOS formulation for two simple illustrative models and show that, using standard finite difference discretization of the EOS formulation, we get an accurate and stable representation of the solution to the scattering problems defined by the two toy models. A discussion of the stability of our schemes for both toy models has been relegated to Appendix A. We have found that stability of our scheme requires that the time step is contained in an interval. This interval is determined by the domain-based method, which is propagating the fields inside the scattering object forward in time. While applying the EOS approach to the

case of 3D electromagnetic scattering, we also found a stability interval for the time step. For this case however, we find that both the domain part and the boundary part of the EOS formulation play a role in determining the interval. We believe that the way that the material parameters for the scattering objects influence the boundaries of the stability interval has some interesting things to say about the occurrence of the late time instability from antenna theory.

3 The second scattering model; two way propagation

Our second toy model, model 2 is

$$\begin{aligned}\varphi_t &= \mu_1 \psi_x + j, \\ \psi_t &= \nu_1 \varphi_x, \\ \rho_t &= -j_x, \\ j_t &= (\alpha - \beta \rho) \varphi - \gamma j \quad a_0 < x < a_1,\end{aligned}\tag{3.1}$$

where, like for model 1, $\varphi = \varphi(x, t)$, $j = j(x, t)$ and $\rho(x, t)$ are interpreted as “electric field”, “current density” and “charge density”. The additional field, $\psi(x, t)$ is interpreted as the “magnetic” field. The charge density and current density will, as in model 1, be confined to the interval $[a_0, a_1]$ on the real axis whereas the fields φ and ψ are defined on the whole real axis. The interval $[a_0, a_1]$ is, like for model 1, the analog of a compact scattering object in the electromagnetic situation. Outside the interval the model equations are

$$\begin{aligned}\varphi_t &= \mu_0 \psi_x + j_s, \\ \psi_t &= \nu_0 \varphi_x,\end{aligned}\tag{3.2}$$

where the function $j_s(x, t)$ is a given source that, like for model 1, has its support on a compact set in the interval $x > a_1$. The parameters $\mu_1, \mu_0, \nu_1, \nu_0$ are "material" parameters. Using the translation $\mu \rightarrow \frac{1}{\epsilon}$ and $\nu \rightarrow \frac{1}{\mu}$ they are analogous for the electric permittivity, ϵ , and the magnetic permeability, μ , inside and outside the scattering object.

3.1 EOS formulation

In order to derive the EOS formulation for model 2 (3.1),(3.2), we will firstly need a space-time integral identity involving the matrix operator

$$L = \begin{pmatrix} \partial_t & -\mu \partial_x \\ -\nu \partial_x & \partial_t \end{pmatrix},$$

where μ and ν are constants. The operator acts on vector valued functions in the usual way

$$L \begin{pmatrix} \varphi \\ \psi \end{pmatrix} = \begin{pmatrix} \partial_t \varphi - \mu \partial_x \psi \\ \partial_t \psi - \nu \partial_x \varphi \end{pmatrix}.$$

Using integration by parts, it is easy to derive

$$\begin{aligned}
& \int_{S \times T} A \mathcal{L} \begin{pmatrix} \varphi \\ \psi \end{pmatrix} (x, t) dx dt \\
&= \int_{S \times T} \begin{pmatrix} -\partial_t A_{11} + \nu \partial_x A_{12} & \mu \partial_x A_{11} - \partial_t A_{12} \\ -\partial_t A_{21} + \nu \partial_x A_{22} & \mu \partial_x A_{21} - \partial_t A_{22} \end{pmatrix} \begin{pmatrix} \varphi \\ \psi \end{pmatrix} (x, t) dx dt \\
&+ \int_S \begin{pmatrix} A_{11} & A_{12} \\ A_{21} & A_{22} \end{pmatrix} \begin{pmatrix} \varphi \\ \psi \end{pmatrix} (x, t) \Big|_{t_0}^{t_1} dx \\
&+ \int_T \begin{pmatrix} -\nu A_{12} & -\mu A_{11} \\ -\nu A_{22} & -\mu A_{21} \end{pmatrix} \begin{pmatrix} \varphi \\ \psi \end{pmatrix} (x, t) \Big|_{x_0}^{x_1} dt,
\end{aligned}$$

so we get the following integral identity

$$\begin{aligned}
& \int_{S \times T} dx dt \{ A L \begin{pmatrix} \varphi \\ \psi \end{pmatrix} (x, t) - L^\dagger A \begin{pmatrix} \varphi \\ \psi \end{pmatrix} (x, t) \} \\
&= \int_S dx A \begin{pmatrix} \varphi \\ \psi \end{pmatrix} (x, t) \Big|_{t_0}^{t_1} + \int_T dt B \begin{pmatrix} \varphi \\ \psi \end{pmatrix} (x, t) \Big|_{x_0}^{x_1}, \tag{3.3}
\end{aligned}$$

where $S = (x_0, x_1)$ and $T = (t_0, t_1)$ are open space and time intervals and where φ and ψ are smooth functions on the space-time interval $S \times T$. Also $A = A(x, t)$ is a 2×2 matrix valued function and L^\dagger is the formal adjoint to the operator L , and acts on the matrix valued function A in the following way

$$L^\dagger A = \begin{pmatrix} -\partial_t A_{11} + \nu \partial_x A_{12} & \mu \partial_x A_{11} - \partial_t A_{12} \\ -\partial_t A_{21} + \nu \partial_x A_{22} & \mu \partial_x A_{21} - \partial_t A_{22} \end{pmatrix}. \tag{3.4}$$

B is the 2×2 matrix valued function

$$B = \begin{pmatrix} -\nu A_{12} & -\mu A_{11} \\ -\nu A_{22} & -\mu A_{21} \end{pmatrix}. \tag{3.5}$$

The second item we need in order to derive the EOS formulation for model (3.1), (3.2), is the advanced Green's function for the operator L^\dagger . This is a 2×2 matrix valued function $G(x, t, x', t')$ that satisfies the equation

$$L^\dagger G(x, t, x', t') = \delta(t - t') \delta(x - x') I, \tag{3.6}$$

and that vanishes for $t > t'$. In (3.6), I is the 2×2 identity matrix. Due to the fact that any Green's function, because of translational invariance only depends on $x - x'$ and $t - t'$, we can solve

$$L^\dagger G(x, t) = \delta(t) \delta(x) I,$$

instead. Writing out components we get

$$\begin{aligned}
\partial_t G_{11} - \nu \partial_x G_{12} &= -\delta(t) \delta(x), \\
\partial_t G_{12} - \mu \partial_x G_{11} &= 0, \\
\partial_t G_{21} - \nu \partial_x G_{22} &= 0, \\
\partial_t G_{22} - \mu \partial_x G_{21} &= -\delta(t) \delta(x).
\end{aligned} \tag{3.7}$$

Performing Fourier transform (2.5) on the first two equations of (3.7) gives

$$\begin{aligned} -i\omega\hat{G}_{11} - i\nu k\hat{G}_{12} &= -1, \\ -i\omega\hat{G}_{12} - i\nu k\hat{G}_{11} &= 0. \end{aligned} \quad (3.8)$$

The solutions to (3.8) are

$$\begin{aligned} \hat{G}_{11}(k, \omega) &= \frac{-i\omega}{\omega^2 - c^2k^2}, \\ \hat{G}_{12}(k, \omega) &= \frac{i\mu k}{\omega^2 - c^2k^2}, \end{aligned} \quad (3.9)$$

where $c^2 = \mu\nu$. By enforcing the inverse Fourier transform (2.6) on (3.9), we get

$$\begin{aligned} G_{11}(x, t) &= \frac{1}{4\pi^2} \int_{-\infty}^{\infty} g_{11}(k, t) e^{ikx} dk, \\ G_{12}(x, t) &= \frac{1}{4\pi^2} \int_{-\infty}^{\infty} g_{12}(k, t) e^{ikx} dk, \end{aligned} \quad (3.10)$$

where

$$\begin{aligned} g_{11}(k, t) &= \int_{-\infty}^{\infty} \hat{G}_{11}(k, \omega) e^{-i\omega t} d\omega, \\ g_{12}(k, t) &= \int_{-\infty}^{\infty} \hat{G}_{12}(k, \omega) e^{-i\omega t} d\omega. \end{aligned}$$

The expressions for g_{11} and g_{12} are not really well defined since the integrands have two poles on the real ω -axis, so we choose the advanced Green's function for our work. It is defined by shifting the integral contour from the real ω -axis to a contour below and parallel to the real axis at a distance $c_\epsilon : z = \omega - i\epsilon, \epsilon > 0$, thus

$$\begin{aligned} g_{11}(k, t) &= \int_{c_\epsilon} \frac{-iz}{z^2 - c^2k^2} e^{-izt} dz, \\ g_{12}(k, t) &= \int_{c_\epsilon} \frac{i\mu k}{z^2 - c^2k^2} e^{-izt} dz. \end{aligned}$$

If $t > 0$,

$$\lim_{z_i \rightarrow -\infty} e^{z_i t} = 0,$$

so we close the contour in the lower half plane and have

$$\begin{aligned} g_{11}(k, t) &= 0, \\ g_{12}(k, t) &= 0. \end{aligned}$$

If $t < 0$,

$$\lim_{z_i \rightarrow +\infty} e^{z_i t} = 0,$$

then we close the contour in the upper half plane. There are now two poles $z = \pm ck$ inside the closed contour. Cauchy's residue theorem gives

$$\begin{aligned} g_{11}(k, t) &= \pi \{ e^{ikct} + e^{-ikct} \}, \\ g_{12}(k, t) &= \frac{\pi\mu}{c} \{ e^{ikct} - e^{-ikct} \}. \end{aligned} \quad (3.11)$$

Inserting (3.11) into (3.10), we obtain

$$\begin{aligned} G_{11}(k, t) &= \frac{\theta(-t)}{2}(\delta(x+ct) + \delta(x-ct)), \\ G_{12}(k, t) &= \frac{\mu\theta(-t)}{2c}(\delta(x+ct) - \delta(x-ct)). \end{aligned}$$

G_{12} and G_{22} are calculated in the same way,

$$\begin{aligned} G_{21}(k, t) &= \frac{\nu\theta(-t)}{2c}(\delta(x+ct) - \delta(x-ct)), \\ G_{22}(k, t) &= \frac{\theta(-t)}{2}(\delta(x+ct) + \delta(x-ct)). \end{aligned}$$

In the end, G is given by

$$\begin{aligned} G(x, t, x', t') &= \frac{\theta(t' - t)}{2c} \left\{ \begin{pmatrix} c & \mu \\ \nu & c \end{pmatrix} \delta(x - x' + c(t - t')) \right. \\ &\quad \left. + \begin{pmatrix} c & -\mu \\ -\nu & c \end{pmatrix} \delta(x - x' - c(t - t')) \right\}, \end{aligned} \quad (3.12)$$

where $\theta(s)$ is the Heaviside step function. Note that, using the identifications introduced while describing model 2 at the start of the current section, the formula defining the speed, c , is completely analogous to the one defining the speed of light in electromagnetics.

We will now apply the integral identity (3.3) to each space interval $(-\infty, a_0)$, (a_0, a_1) and (a_1, ∞) with A equal to the advanced Green's function (3.12) for the corresponding interval and where φ and ψ are solutions to the system (3.1), (3.2) with vanishing initial conditions $\varphi(x, t_0) = \psi(x, t_0) = 0$.

For the first interval, $(-\infty, a_0)$, we let A be the Green's function

$$\begin{aligned} G_0(x, t, x', t') &= \frac{\theta(t' - t)}{2c_0} \left\{ \begin{pmatrix} c_0 & \mu_0 \\ \nu_0 & c_0 \end{pmatrix} \delta(x - x' + c_0(t - t')) \right. \\ &\quad \left. + \begin{pmatrix} c_0 & -\mu_0 \\ -\nu_0 & c_0 \end{pmatrix} \delta(x - x' - c_0(t - t')) \right\}, \end{aligned} \quad (3.13)$$

where $c_0^2 = \mu_0\nu_0$. In this interval we let $\varphi = \varphi_0, \psi = \psi_0$ be the solution to the system

$$\begin{aligned} \varphi_{0t} &= \mu_0\psi_{0x}, \\ \psi_{0t} &= \nu_0\varphi_{0x}, \\ &\Downarrow \\ L_0 \begin{pmatrix} \varphi_0 \\ \psi_0 \end{pmatrix} &= 0. \end{aligned} \quad (3.14)$$

Inserting (3.13), (3.14) and $S = (-\infty, a_0)$ into the integral identity (3.3), using the initial conditions and the fact that the Green's function is advanced, we get

for x in the interval $(-\infty, a_0)$.

$$\begin{aligned} \begin{pmatrix} \varphi_0 \\ \psi_0 \end{pmatrix} (x, t) &= - \int_{t_0}^{t_1} dt' B_0(a_0, t', x, t) \begin{pmatrix} \varphi_0 \\ \psi_0 \end{pmatrix} (a_0, t') \\ &+ \lim_{R \rightarrow -\infty} \int_{t_0}^{t_1} dt' B_0(R, t', x, t) \begin{pmatrix} \varphi_0 \\ \psi_0 \end{pmatrix} (R, t'), \end{aligned} \quad (3.15)$$

after interchanging primed and unprimed variables.

The function B_0 is from (3.5)

$$\begin{aligned} B_0(x', t', x, t) &= - \frac{\theta(t-t')}{2} \left\{ \begin{pmatrix} c_0 & \mu_0 \\ \nu_0 & c_0 \end{pmatrix} \delta(x-x' + c_0(t-t')) \right. \\ &+ \left. \begin{pmatrix} -c_0 & \mu_0 \\ \nu_0 & -c_0 \end{pmatrix} \delta(x-x' - c_0(t-t')) \right\}. \end{aligned} \quad (3.16)$$

From (3.16) it is evident that the last term in (3.15) vanishes. This is because for large enough R , the argument of the delta function does not change sign in the interval of integration. Inserting the expression (3.16) into (3.15) and changing to the variable defining the argument of the delta function in the two integrals, we get that for x in $(-\infty, a_0)$

$$\begin{pmatrix} \varphi_0 \\ \psi_0 \end{pmatrix} (x, t) = \frac{\theta(x-a_0 + c_0(t-t_0))}{2c_0} \begin{pmatrix} c_0 & \mu_0 \\ \nu_0 & c_0 \end{pmatrix} \begin{pmatrix} \varphi_0 \\ \psi_0 \end{pmatrix} (a_0, t + \frac{x-a_0}{c_0}). \quad (3.17)$$

For the second interval, (a_0, a_1) , we let A be the Green's function

$$\begin{aligned} G_1(x, t, x', t') &= \frac{\theta(t'-t)}{2c_1} \left\{ \begin{pmatrix} c_1 & \mu_1 \\ \nu_1 & c_1 \end{pmatrix} \delta(x-x' + c_1(t-t')) \right. \\ &+ \left. \begin{pmatrix} c_1 & -\mu_1 \\ -\nu_1 & c_1 \end{pmatrix} \delta(x-x' - c_1(t-t')) \right\}. \end{aligned} \quad (3.18)$$

where $c_1^2 = \mu_1 \nu_1$. In this interval, the functions $\varphi = \varphi_1, \psi = \psi_1$ are the solutions to the system

$$\begin{aligned} \varphi_{1t} &= \mu_1 \psi_{1x} + j, \\ \psi_{1t} &= \nu_1 \varphi_{1x}, \\ &\Downarrow \\ L_1 \begin{pmatrix} \varphi_1 \\ \psi_1 \end{pmatrix} &= \begin{pmatrix} j \\ 0 \end{pmatrix}. \end{aligned} \quad (3.19)$$

Inserting (3.18), (3.19) and $S = (a_0, a_1)$ in the integral identity (3.3), using the vanishing initial conditions and the fact that the Green's function is advanced,

we get for x in the interval (a_0, a_1) .

$$\begin{aligned} \begin{pmatrix} \varphi_1 \\ \psi_1 \end{pmatrix} (x, t) &= \int_{S \times T} dx' dt' G_1(x', t', x, t) \begin{pmatrix} j \\ 0 \end{pmatrix} (x', t') \\ &\quad - \int_{t_0}^{t_1} dt' B_1(a_1, t', x, t) \begin{pmatrix} \varphi_1 \\ \psi_1 \end{pmatrix} (a_1, t) \\ &\quad + \int_{t_0}^{t_1} dt' B_1(a_0, t', x, t) \begin{pmatrix} \varphi_1 \\ \psi_1 \end{pmatrix} (a_0, t), \end{aligned} \quad (3.20)$$

after interchanging primed and unprimed variables.

The function B_1 is from (3.5)

$$\begin{aligned} B_1(x', t', x, t) &= -\frac{\theta(t-t')}{2} \left\{ \begin{pmatrix} c_1 & \mu_1 \\ \nu_1 & c_1 \end{pmatrix} \delta(x-x'+c_1(t-t')) \right. \\ &\quad \left. + \begin{pmatrix} -c_1 & \mu_1 \\ \nu_1 & -c_1 \end{pmatrix} \delta(x-x'-c_1(t-t')) \right\}. \end{aligned} \quad (3.21)$$

Inserting (3.18) and (3.21) into (3.20), we get after changing variables to the arguments in the delta functions that for x in (a_0, a_1)

$$\begin{aligned} \begin{pmatrix} \varphi_1 \\ \psi_1 \end{pmatrix} (x, t) &= \\ &\frac{1}{2c_1^2} \begin{pmatrix} c_1 & -\mu_1 \\ -\nu_1 & c_1 \end{pmatrix} \int_{a_0}^x dx' \theta(c_1(t-t_0) - (x-x')) \begin{pmatrix} j \\ 0 \end{pmatrix} (x', t - \frac{x-x'}{c_1}) \\ &+ \frac{1}{2c_1^2} \begin{pmatrix} c_1 & \mu_1 \\ \nu_1 & c_1 \end{pmatrix} \int_x^{a_1} dx' \theta(c_1(t-t_0) - (x'-x)) \begin{pmatrix} j \\ 0 \end{pmatrix} (x', t - \frac{x'-x}{c_1}) \\ &+ \theta(c_1(t-t_0) - (a_1-x)) \frac{1}{2c_1} \begin{pmatrix} c_1 & \mu_1 \\ \nu_1 & c_1 \end{pmatrix} \begin{pmatrix} \varphi_1 \\ \psi_1 \end{pmatrix} (a_1, t - \frac{a_1-x}{c_1}) \\ &- \theta(c_1(t-t_0) - (x-a_0)) \frac{1}{2c_1} \begin{pmatrix} -c_1 & \mu_1 \\ \nu_1 & -c_1 \end{pmatrix} \begin{pmatrix} \varphi_1 \\ \psi_1 \end{pmatrix} (a_0, t - \frac{x-a_0}{c_1}). \end{aligned} \quad (3.22)$$

For the third interval, (a_1, ∞) , we let A be the Green's function

$$\begin{aligned} G_0(x, t, x', t') &= \frac{\theta(t'-t)}{2c_0} \left\{ \begin{pmatrix} c_0 & \mu_0 \\ \nu_0 & c_0 \end{pmatrix} \delta(x-x'+c_0(t-t')) \right. \\ &\quad \left. + \begin{pmatrix} c_0 & -\mu_0 \\ -\nu_0 & c_0 \end{pmatrix} \delta(x-x'-c_0(t-t')) \right\}. \end{aligned} \quad (3.23)$$

In this interval, the functions $\varphi = \varphi_2, \psi = \psi_2$ are the solutions to the system

$$\begin{aligned} \varphi_{2t} &= \mu_0 \psi_{2x} + j_s, \\ \psi_{2t} &= \nu_0 \varphi_{2x}, \\ &\Downarrow \\ L_0 \begin{pmatrix} \varphi_2 \\ \psi_2 \end{pmatrix} &= \begin{pmatrix} j_s \\ 0 \end{pmatrix}. \end{aligned} \quad (3.24)$$

Inserting (3.23), (3.24) and $S = (a_1, \infty)$ in the integral identity (3.3), using the initial conditions and the fact that the Green's function is advanced, we get for x in the interval (a_1, ∞) .

$$\begin{aligned} \begin{pmatrix} \varphi_2 \\ \psi_2 \end{pmatrix} (x, t) &= \int_{S \times T} dx' dt' G_0(x', t', x, t) \begin{pmatrix} j_s \\ 0 \end{pmatrix} (x', t') \\ &\quad - \lim_{R \rightarrow \infty} \int_{t_0}^{t_1} dt' B_0(R, t', x, t) \begin{pmatrix} \varphi_2 \\ \psi_2 \end{pmatrix} (R, t) \\ &\quad + \int_{t_0}^{t_1} dt' B_0(a_1, t', x, t) \begin{pmatrix} \varphi_2 \\ \psi_2 \end{pmatrix} (a_1, t), \end{aligned} \quad (3.25)$$

after interchanging primed and unprimed variables.

Since the arguments of the delta functions in B_0 does not change sign in the interval of integration, for R big enough, it is clear that the second term in (3.25) will vanish. Inserting (3.23) and (3.16) into the remaining terms of (3.25), we get after changing variables to the arguments in the delta functions that for x in (a_1, ∞)

$$\begin{aligned} \begin{pmatrix} \varphi_2 \\ \psi_2 \end{pmatrix} (x, t) &= \\ &\quad - \theta(c_0(t - t_0) - (x - a_1)) \frac{1}{2c_0} \begin{pmatrix} -c_0 & \mu_0 \\ \nu_0 & -c_0 \end{pmatrix} \begin{pmatrix} \varphi_2 \\ \psi_2 \end{pmatrix} (a_1, t - \frac{x - a_1}{c_0}) \\ &\quad + \begin{pmatrix} \varphi_i \\ \psi_i \end{pmatrix} (x, t), \end{aligned} \quad (3.26)$$

where φ_i and ψ_i are fields that are entirely determined by the given source j_s

$$\begin{aligned} \begin{pmatrix} \varphi_i \\ \psi_i \end{pmatrix} (x, t) &= \\ &\quad \frac{1}{2c_0^2} \begin{pmatrix} c_0 & -\mu_0 \\ -\nu_0 & c_0 \end{pmatrix} \int_{a_1}^x dx' \theta(c_0(t - t_0) - (x - x')) \begin{pmatrix} j_s \\ 0 \end{pmatrix} (x', t - \frac{x - x'}{c_0}) \\ &\quad + \frac{1}{2c_0^2} \begin{pmatrix} c_0 & \mu_0 \\ \nu_0 & c_0 \end{pmatrix} \int_x^\infty dx' \theta(c_0(t - t_0) - (x' - x)) \begin{pmatrix} j_s \\ 0 \end{pmatrix} (x', t - \frac{x' - x}{c_0}). \end{aligned}$$

Taking the limit of the integral identities (3.17), (3.22) and (3.26) as x approaches

the boundary points $\{a_0, a_1\}$ from inside and outside the interval (a_0, a_1) we get

$$\begin{pmatrix} c_0 & -\mu_0 \\ -\nu_0 & c_0 \end{pmatrix} \begin{pmatrix} \varphi_0 \\ \psi_0 \end{pmatrix} (a_0, t) = 0, \quad (3.27)$$

$$\begin{pmatrix} c_1 & \mu_1 \\ \nu_1 & c_1 \end{pmatrix} \begin{pmatrix} \varphi_1 \\ \psi_1 \end{pmatrix} (a_0, t) =$$

$$\begin{aligned} & \frac{1}{c_1} \begin{pmatrix} c_1 & \mu_1 \\ \nu_1 & c_1 \end{pmatrix} \int_{a_0}^{a_1} dx' \theta(c_1(t-t_0) - (x' - a_0)) \begin{pmatrix} j \\ 0 \end{pmatrix} (x', t - \frac{x' - a_0}{c_1}) \\ & + \theta(c_1(t-t_0) - (a_1 - a_0)) \begin{pmatrix} c_1 & \mu_1 \\ \nu_1 & c_1 \end{pmatrix} \begin{pmatrix} \varphi_1 \\ \psi_1 \end{pmatrix} (a_1, t - \frac{a_1 - a_0}{c_1}), \quad (3.28) \end{aligned}$$

$$\begin{pmatrix} c_1 & -\mu_1 \\ -\nu_1 & c_1 \end{pmatrix} \begin{pmatrix} \varphi_1 \\ \psi_1 \end{pmatrix} (a_1, t) =$$

$$\begin{aligned} & \frac{1}{c_1} \begin{pmatrix} c_1 & -\mu_1 \\ -\nu_1 & c_1 \end{pmatrix} \int_{a_0}^{a_1} dx' \theta(c_1(t-t_0) - (a_1 - x')) \begin{pmatrix} j \\ 0 \end{pmatrix} (x', t - \frac{a_1 - x'}{c_1}) \\ & - \theta(c_1(t-t_0) - (a_1 - a_0)) \begin{pmatrix} -c_1 & \mu_1 \\ \nu_1 & -c_1 \end{pmatrix} \begin{pmatrix} \varphi_1 \\ \psi_1 \end{pmatrix} (a_0, t - \frac{a_1 - a_0}{c_1}), \quad (3.29) \end{aligned}$$

$$\begin{pmatrix} c_0 & \mu_0 \\ \nu_0 & c_0 \end{pmatrix} \begin{pmatrix} \varphi_2 \\ \psi_2 \end{pmatrix} (a_1, t) = 2c_0 \begin{pmatrix} \varphi_i \\ \psi_i \end{pmatrix} (a_1, t). \quad (3.30)$$

Continuity of the fields at the boundary points $\{a_0, a_1\}$, gives us two additional equations,

$$\begin{pmatrix} \varphi_0 \\ \psi_0 \end{pmatrix} (a_0, t) = \begin{pmatrix} \varphi_1 \\ \psi_1 \end{pmatrix} (a_0, t), \quad (3.31)$$

$$\begin{pmatrix} \varphi_1 \\ \psi_1 \end{pmatrix} (a_1, t) = \begin{pmatrix} \varphi_2 \\ \psi_2 \end{pmatrix} (a_1, t). \quad (3.32)$$

Altogether we have six linear equations for the four vectors

$$\begin{pmatrix} \varphi_0 \\ \psi_0 \end{pmatrix} (a_0, t), \begin{pmatrix} \varphi_1 \\ \psi_1 \end{pmatrix} (a_0, t), \begin{pmatrix} \varphi_1 \\ \psi_1 \end{pmatrix} (a_1, t), \begin{pmatrix} \varphi_2 \\ \psi_2 \end{pmatrix} (a_1, t).$$

Thus our system (3.27)-(3.32) is overdetermined just like it was for model 1. And just like for model 1, the system (3.27)-(3.32) contains equations that are redundant. Mathematically this is reflected in the fact that the determinant of the matrices

$$\begin{pmatrix} c_j & \pm\mu_j \\ \pm\nu_j & c_j \end{pmatrix}, \quad j = 0, 1,$$

are all zero. For the first toy model, it was obvious which two equations were redundant. Here it is not immediately clear which equations we can remove, and

this will also be the case if we write down the EOS formulation for more general systems of PDEs, like for example Maxwell's equations. For the system (3.27)-(3.32), it is not very difficult to identify the redundant equations, but we would rather introduce a different approach that is generally quite useful when working with the EOS formulations of PDEs. This is the method that has been used by the research community to calculate electromagnetic scattering from linear homogeneous scattering objects using a time dependent integral formulation of Maxwell's equations. The *reason* that this method has been used for Maxwell's equations has not been clearly stated in the research literature. It has taken the form of a trick that is needed to achieve stability and accuracy for the numerical implementation of the boundary formulation of electromagnetic scattering.

The point is that, although the system (3.27)-(3.32) is singular, we know from its construction that it has a solution consisting boundary values coming from the unique solution to the system (3.1),(3.2).

In terms of linear algebra, the situation is that for two given singular matrices A and B , the system

$$\begin{aligned} A\mathbf{x} &= \mathbf{b}_1, \\ B\mathbf{x} &= \mathbf{b}_2, \end{aligned} \tag{3.33}$$

has a solution, \mathbf{x} . Let us assume that there are numbers a and b such that

$$\det(aA + bB) \neq 0.$$

Given (3.33) it is clear that \mathbf{x} is a solution to the linear system

$$(aA + bB)\mathbf{x} = a\mathbf{b}_1 + b\mathbf{b}_2, \tag{3.34}$$

and since the system (3.34) is nonsingular, \mathbf{x} is the unique solution to the system. Finding numbers such that $aA + bB$ is nonsingular is in general not difficult.

Let us apply this approach to the system (3.27)-(3.32). Simply adding together the equations give us a matrix

$$\begin{pmatrix} c_0 & -\mu_0 \\ -\nu_0 & c_0 \end{pmatrix} + \begin{pmatrix} c_1 & \mu_1 \\ \nu_1 & c_1 \end{pmatrix} = \begin{pmatrix} c_1 + c_0 & \mu_1 - \mu_0 \\ \nu_1 - \nu_0 & c_1 + c_0 \end{pmatrix},$$

and

$$\det \begin{pmatrix} c_1 + c_0 & \mu_1 - \mu_0 \\ \nu_1 - \nu_0 & c_1 + c_0 \end{pmatrix} = 2c_1c_0 + \mu_0\nu_1 + \mu_1\nu_0,$$

which is nonzero since all the numbers ν_i, μ_j, c_j are positive by assumption. In a similar way, adding together (3.29) and (3.30) will result in a nonsingular system. Thus from the singular system (3.27)-(3.32) we get the nonsingular system

$$\begin{aligned} & \begin{pmatrix} c_1 + c_0 & \mu_1 - \mu_0 \\ \nu_1 - \nu_0 & c_1 + c_0 \end{pmatrix} \begin{pmatrix} \varphi_1 \\ \psi_1 \end{pmatrix} (a_0, t) = \\ & \frac{1}{c_1} \begin{pmatrix} c_1 & \mu_1 \\ \nu_1 & c_1 \end{pmatrix} \int_{a_0}^{a_1} dx' \theta(c_1(t - t_0) - (x' - a_0)) \begin{pmatrix} j \\ 0 \end{pmatrix} (x', t - \frac{x' - a_0}{c_1}) \\ & + \theta(c_1(t - t_0) - (a_1 - a_0)) \begin{pmatrix} c_1 & \mu_1 \\ \nu_1 & c_1 \end{pmatrix} \begin{pmatrix} \varphi_1 \\ \psi_1 \end{pmatrix} (a_1, t - \frac{a_1 - a_0}{c_1}), \end{aligned} \tag{3.35}$$

$$\begin{aligned}
& \begin{pmatrix} c_0 + c_1 & \mu_0 - \mu_1 \\ \nu_0 - \nu_1 & c_1 + c_0 \end{pmatrix} \begin{pmatrix} \varphi_1 \\ \psi_1 \end{pmatrix} (a_1, t) = \\
& \frac{1}{c_1} \begin{pmatrix} c_1 & -\mu_1 \\ -\nu_1 & c_1 \end{pmatrix} \int_{a_0}^{a_1} dx' \theta(c_1(t - t_0) - (a_1 - x')) \begin{pmatrix} j \\ 0 \end{pmatrix} (x', t - \frac{a_1 - x'}{c_1}) \\
& - \theta(c_1(t - t_0) - (a_1 - a_0)) \begin{pmatrix} -c_1 & \mu_1 \\ \nu_1 & -c_1 \end{pmatrix} \begin{pmatrix} \varphi_1 \\ \psi_1 \end{pmatrix} (a_0, t - \frac{a_1 - a_0}{c_1}) \\
& + 2c_0 \begin{pmatrix} \varphi_i \\ \psi_i \end{pmatrix} (a_1, t). \tag{3.36}
\end{aligned}$$

The system (3.35), (3.36), which determine the boundary values of the fields in term of internal and external current densities, together with the differential equations (3.1), restricted to the inside the scattering object (a_0, a_1) , constitute the EOS formulation for model 2.

3.2 Numerical implementation of the EOS formulation

The numerical implementation of model 2 contains the same elements as the ones we introduced for model 1. Thus we first define a nonuniform space grid inside the scattering object, (a_0, a_1) ,

$$x_i = a_0 + (i + 0.5)\Delta x, \quad i = 0, 1, \dots, N - 1, \tag{3.37}$$

where $\Delta x = \frac{a_1 - a_0}{N}$. The grid points (3.37) are the internal nodes for model 2. We also introduce the discrete time grid

$$t^n = n\Delta t, \quad n = 0, 1, \dots.$$

The values of the parameter Δt will of course, like for model 1, be bounded by the requirement of stability for the scheme. We apply the Lax-Wendroff method to the first three equations of (3.1) and the modified Euler's method to the last equation of (3.1). For interval (a_0, a_1) , the numerical iteration can be written as

$$\begin{aligned}
\varphi_i^{n+1} &= \varphi_i^n + \Delta t (\mu_1 \frac{\partial \psi}{\partial x})_i^n + \frac{1}{2} (\Delta t)^2 (\mu_1 \nu_1 \frac{\partial^2 \varphi}{\partial x^2} + f)_i^n, \\
\psi_i^{n+1} &= \psi_i^n + \Delta t (\nu_1 \frac{\partial \varphi}{\partial x})_i^n + \frac{1}{2} (\Delta t)^2 (\mu_1 \nu_1 \frac{\partial^2 \psi}{\partial x^2} + \nu_1 \frac{\partial j}{\partial x})_i^n, \\
\rho_i^{n+1} &= \rho_i^n + \Delta t (-\frac{\partial j}{\partial x})_i^n + \frac{1}{2} (\Delta t)^2 (-\frac{\partial f}{\partial x})_i^n, \\
\bar{j}_i^{n+1} &= j_i^n + \Delta t f_i^n, \\
j_i^{n+1} &= \frac{1}{2} (j_i^n + \bar{j}_i^n + \Delta t f(\rho_i^{n+1}, \varphi_i^{n+1}, \bar{j}_i^{n+1})),
\end{aligned} \tag{3.38}$$

where $f = (\alpha - \beta\rho)\varphi - \gamma j$. The finite difference approximations for the fields and the current density at all internal nodes, except the two nodes closest to

the boundary points a_0 and a_1 , are given by the standard expressions

$$\begin{aligned} \left(\frac{\partial\phi}{\partial x}\right)_i^n &= \frac{\phi_{i+1}^n - \phi_{i-1}^n}{2\Delta x}, \\ \left(\frac{\partial^2\phi}{\partial x^2}\right)_i^n &= \frac{\phi_{i+1}^n - 2\phi_i^n + \phi_{i-1}^n}{(\Delta x)^2}, \quad \phi = \varphi, \psi, j, \end{aligned} \quad (3.39)$$

for $i = 1, 2, \dots, N-2$. For the two internal nodes closest to the boundary points, we need to use alternative difference rules because the grid is nonuniform in the domain around these nodes

$$\begin{aligned} \left(\frac{\partial\phi}{\partial x}\right)_0^n &= -\frac{1}{3 \cdot \Delta x} (4\phi_{a_0}^n - 3\phi_0^n - \phi_1^n), \\ \left(\frac{\partial^2\phi}{\partial x^2}\right)_0^n &= \frac{4}{3 \cdot (\Delta x)^2} (2\phi_{a_0}^n - 3\phi_0^n + \phi_1^n), \\ \left(\frac{\partial\phi}{\partial x}\right)_{N-1}^n &= \frac{1}{3 \cdot \Delta x} (4\phi_{a_1}^n - 3\phi_{N-1}^n - \phi_{N-2}^n), \\ \left(\frac{\partial^2\phi}{\partial x^2}\right)_{N-1}^n &= \frac{4}{3 \cdot (\Delta x)^2} (2\phi_{a_1}^n - 3\phi_{N-1}^n + \phi_{N-2}^n), \\ \left(\frac{\partial j}{\partial x}\right)_0^n &= \frac{1}{2\Delta x} (4j_1^n - 3j_0^n - j_2^n), \\ \left(\frac{\partial j}{\partial x}\right)_{N-1}^n &= -\frac{1}{2\Delta x} (4j_{N-2}^n - 3j_{N-1}^n - j_{N-3}^n), \end{aligned} \quad (3.40)$$

where $\phi = \varphi, \psi$. The discretization of the boundary update rules (3.35) and (3.36) are

$$\begin{aligned} &\begin{pmatrix} c_1 + c_0 & \mu_1 - \mu_0 \\ \nu_1 - \nu_0 & c_1 + c_0 \end{pmatrix} \begin{pmatrix} \varphi \\ \psi \end{pmatrix} (a_0, t_{n+1}) \\ &= \frac{\Delta x}{c_1} \begin{pmatrix} c_1 & \mu_1 \\ \nu_1 & c_1 \end{pmatrix} \sum_{i=0}^{N-1} \theta(t_{n+1} - t_0 - \frac{x_i - a_0}{c_1}) \begin{pmatrix} j \\ 0 \end{pmatrix} (x_i, t_{n+1} - \frac{x_i - a_0}{c_1}) \end{aligned} \quad (3.41)$$

$$\begin{aligned} &+ \begin{pmatrix} c_1 & \mu_1 \\ \nu_1 & c_1 \end{pmatrix} \theta(t_{n+1} - t_0 - \frac{a_1 - a_0}{c_1}) \begin{pmatrix} \varphi \\ \psi \end{pmatrix}_- (a_1, t_{n+1} - \frac{a_1 - a_0}{c_1}), \\ &\begin{pmatrix} c_1 + c_0 & \mu_0 - \mu_1 \\ \nu_0 - \nu_1 & c_1 + c_0 \end{pmatrix} \begin{pmatrix} \varphi \\ \psi \end{pmatrix} (a_1, t_{n+1}) = \\ &\frac{\Delta x}{c_1} \begin{pmatrix} c_1 & -\mu_1 \\ -\nu_1 & c_1 \end{pmatrix} \sum_{i=0}^{N-1} \theta(t_{n+1} - t_0 - \frac{a_1 - x_i}{c_1}) \begin{pmatrix} j \\ 0 \end{pmatrix} (x_i, t_{n+1} - \frac{a_1 - x_i}{c_1}) \\ &- \begin{pmatrix} -c_1 & \mu_1 \\ \nu_1 & -c_1 \end{pmatrix} \theta(t_{n+1} - t_0 - \frac{a_1 - a_0}{c_1}) \begin{pmatrix} \varphi \\ \psi \end{pmatrix}_+ (a_0, t_{n+1} - \frac{a_1 - a_0}{c_1}) \quad (3.42) \\ &+ 2c_0 \begin{pmatrix} \varphi_i \\ \psi_i \end{pmatrix} (a_1, t_{n+1}). \end{aligned}$$

where $\begin{pmatrix} \varphi_i \\ \psi_i \end{pmatrix}(a_1, t_{n+1})$ are determined by the external source. The iteration (3.38) with the boundary update rules (3.41), (3.42) supplemented by the finite difference rules (3.39) and (3.40) constitute our numerical implementation of the EOS formulation for model 2.

3.3 Artificial source test

The source extended model 2, is given by

$$\begin{aligned}\varphi_t &= \mu_1 \psi_x + j + g_1, \\ \psi_t &= \nu_1 \varphi_x + g_2, \\ \rho_t &= -j_x + g_3, \\ j_t &= (\alpha - \beta \rho) \varphi - \gamma j + g_4.\end{aligned}$$

For the source extended model 2, any given set of functions $\hat{\varphi}$, $\hat{\psi}$, \hat{j} and $\hat{\rho}$ is a solution if the sources are chosen to be

$$\begin{aligned}\hat{g}_1 &= \hat{\varphi}_t - \mu_1 \hat{\psi}_x - \hat{j}, \\ \hat{g}_2 &= \hat{\psi}_t - \nu_1 \hat{\varphi}_x, \\ \hat{g}_3 &= \hat{\rho}_t + \hat{j}_x, \\ \hat{g}_4 &= \hat{j}_t - (\alpha - \beta \hat{\rho}) \hat{\varphi} + \gamma \hat{j}.\end{aligned}$$

The boundary update rules for the source extended model 2 are changed into

$$\begin{aligned}& \begin{pmatrix} c_1 + c_0 & \mu_1 - \mu_0 \\ \nu_1 - \nu_0 & c_1 + c_0 \end{pmatrix} \begin{pmatrix} \varphi_1 \\ \psi_1 \end{pmatrix} (a_0, t) = \\ & \frac{1}{c_1} \begin{pmatrix} c_1 & \mu_1 \\ \nu_1 & c_1 \end{pmatrix} \int_{a_0}^{a_1} dx' \theta(c_1(t - t_0) - (x' - a_0)) \begin{pmatrix} j + \hat{g}_1 \\ \hat{g}_2 \end{pmatrix} \left(x', t - \frac{x' - a_0}{c_1}\right) \\ & + \theta(c_1(t - t_0) - (a_1 - a_0)) \begin{pmatrix} c_1 & \mu_1 \\ \nu_1 & c_1 \end{pmatrix} \begin{pmatrix} \varphi_1 \\ \psi_1 \end{pmatrix} \left(a_1, t - \frac{a_1 - a_0}{c_1}\right), \\ & \begin{pmatrix} c_0 + c_1 & \mu_0 - \mu_1 \\ \nu_0 - \nu_1 & c_1 + c_0 \end{pmatrix} \begin{pmatrix} \varphi_1 \\ \psi_1 \end{pmatrix} (a_1, t) = \\ & \frac{1}{c_1} \begin{pmatrix} c_1 & -\mu_1 \\ -\nu_1 & c_1 \end{pmatrix} \int_{a_0}^{a_1} dx' \theta(c_1(t - t_0) - (a_1 - x')) \begin{pmatrix} j + \hat{g}_1 \\ \hat{g}_2 \end{pmatrix} \left(x', t - \frac{a_1 - x'}{c_1}\right) \\ & - \theta(c_1(t - t_0) - (a_1 - a_0)) \begin{pmatrix} -c_1 & \mu_1 \\ \nu_1 & -c_1 \end{pmatrix} \begin{pmatrix} \varphi_1 \\ \psi_1 \end{pmatrix} \left(a_0, t - \frac{a_1 - a_0}{c_1}\right) \\ & + 2c_0 \begin{pmatrix} \varphi_i \\ \psi_i \end{pmatrix} (a_1, t).\end{aligned}$$

In Fig 3.1 we compare the numerical and exact solution of the EOS formulation

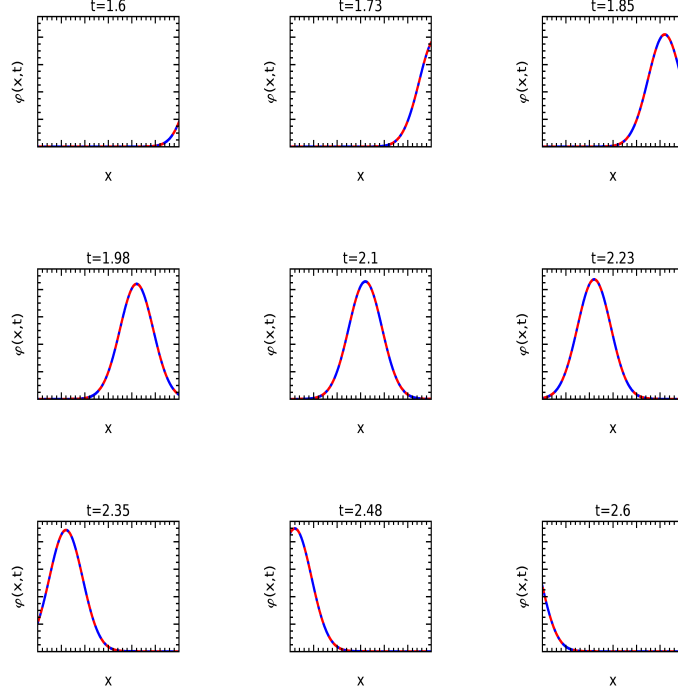


Figure 3.1: Comparison between the numerical solution and the exact solution for the source extended model 2. Parameter values used are $a_0 = 0.0, a_1 = 3.0, N = 1600, \alpha = -1.0, \beta = 0.3, \gamma = 8.0, \mu = 2.0, \nu = 2.0, \mu_0 = 1.0, \nu_0 = 1.0, A_1 = 1.0, A_2 = 1.0, A_3 = 1.0, A_4 = 1.0, b_1 = 1.0, b_2 = 1.0, \alpha_1 = 4.0, \beta_1 = 4.0, \alpha_2 = 4.0, \beta_2 = 4.0, x_o = 6.0, t_s = 1.0, x_j = 1.1, x_\rho = 1.3, t_j = 1.2, t_\rho = 1.3, \delta_1 = 0.3, \delta_2 = 0.32, \delta_3 = 1.0, \delta_4 = 0.33$.

for the source extended model 2. The exact solution we used for this test is

$$\begin{aligned}\hat{\varphi}(x, t) &= \frac{2A_1}{\pi} \arctan(b_1^2 t^2) e^{-\alpha_1(x-x_o+\beta_1(t-t_s))^2}, \\ \hat{\psi}(x, t) &= \frac{2A_2}{\pi} \arctan(b_2^2 t^2) e^{-\alpha_2(x-x_o+\beta_2(t-t_s))^2}, \\ \hat{j}(x, t) &= A_3 e^{-\frac{(x-x_j)^2}{\delta_1^2} - \frac{(t-t_j)^2}{\delta_2^2}}, \\ \hat{\rho}(x, t) &= A_4 e^{-\frac{(x-x_\rho)^2}{\delta_3^2} - \frac{(t-t_\rho)^2}{\delta_4^2}}.\end{aligned}$$

Our implementation clearly passes the artificial source test with flying colors. Fig 3.2 shows scattering of a wave generated by an external source calculated from our numerical implementation of the EOS formulation for model 2. The source we used is given by

$$j_s = A e^{-\alpha_1(x-x_o)^2 - \beta_1(t-t_s)^2}.$$

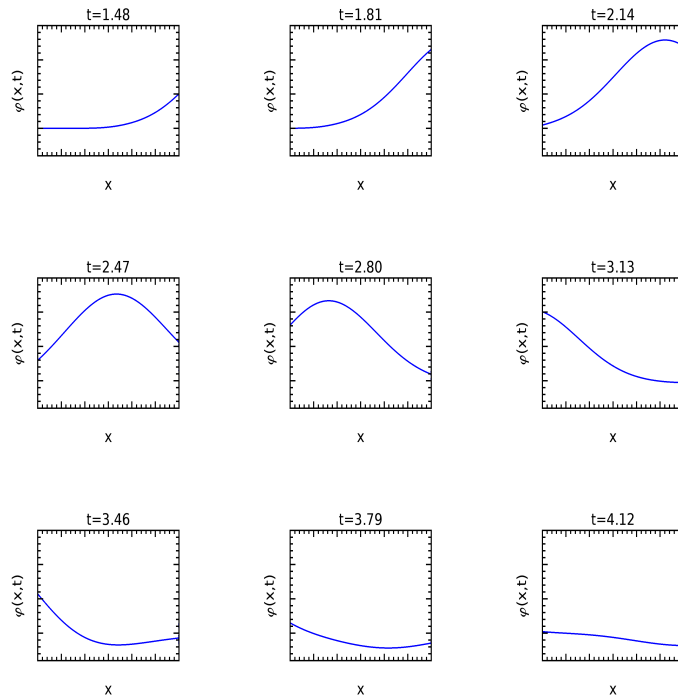


Figure 3.2: A numerical solution of the EOS formulation for model 2 generated by an external source. The parameter values used are $a_0 = 0.0$, $a_1 = 3.0$, $N = 1600$, $\alpha = -1.0$, $\beta = 0.3$, $\gamma = 8.0$, $\mu = 2.0$, $\nu = 2.0$, $\mu_0 = 1.0$, $\nu_0 = 1.0$, $A = 1.0$, $\alpha_1 = 36$, $\beta_1 = 4$, $t_s = 1.0$, $x_o = 4.0$.

A Stability of the numerical schemes for model 1 and model 2

As mentioned in the main text, we do not expect the two 1D models to be representative for stability issues pertaining to numerical implementation to EOS formulations in general. However, there is an issue that is worth discussing here. From the EOS formulation of model 1, one might expect that there would be severe stability issues associated with any numerical approximation. The reason is that the basic equation for the field inside the domain (a_0, a_1)

$$\varphi_t = c_1 \varphi_x, \quad (\text{A.1})$$

uncoupled for simplicity from the internally generated current density j , can only satisfy the boundary condition at the right boundary a_1 induced by the external source. This is because equation (A.1) is of order one in space derivatives. Consequently, one cannot impose any additional boundary condition at a_0 that is independent of the one imposed at a_1 . The EOS formulation evades this problem in this simplified setting by imposing the boundary condition

$$\varphi_1(a_0, t) = \theta(a_0 - a_1 + c_1(t - t_0))\varphi(a_1, t - \frac{a_1 - a_0}{c_1}), \quad (\text{A.2})$$

which depends on the boundary condition at a_1 in exactly the way it needs for a solution, for the boundary value problem for (A.1) on the interval (a_0, a_1) , to exist. However, this existence seems precarious. If we miss the right value by even a small amount in a numerical scheme, are we not then solving a boundary value problem for (A.1) where the two boundary conditions are *not* related in the right way, and is there not a danger that this non-existence will manifest itself in a numerical instability? In fact, could it be that the restricted domain of stability of the EOS formulation, as noted in the main text, is a result of the very particular delay-boundary conditions imposed because of the EOS formulation? If this was true it would be important because such delay boundary conditions are a general feature of EOS formulations. We will however now show that the restricted domain of stability for the 1D models are in fact caused by nonuniformity rather than delayed type boundary conditions.

For this purpose we introduce a family of grids of the interval (a_0, a_1) that are parametrized by ϵ . The grid is uniform for $\epsilon = 0$ and is equal to the nonuniform grid we used for our numerical implementations for model 1 and 2 when $\epsilon = 1$.

$$x_i = a_0 + (i + 1 - 0.5\epsilon)\Delta x, \quad i = 0, 1, \dots, N - 1,$$

where $\epsilon \in [0, 1]$ and

$$\Delta = \frac{N + \epsilon}{N(N + 1)}(a_1 - a_0).$$

To derive a finite difference scheme for (A.1), using the Lax-Wendroff approach, as in the main text, we must to impose some boundary conditions. In the end, these conditions do not influence the stability of the scheme. Therefore, for simplicity, we impose fixed boundary conditions. Given this the numerical scheme takes the form

$$\mathbf{U}_{n+1} = M_1 \mathbf{U}_n + \mathbf{b}, \quad (\text{A.3})$$

where $\mathbf{U} = (\varphi)$ is a N vector, M_1 is a matrix of order $N \times N$ given by

$$M_1 = \begin{bmatrix} \eta_1 + c_1 \eta_2 & \gamma_1 + c_1 \gamma_2 & 0 & 0 & 0 & \dots & 0 \\ \kappa_1 - c_1 \kappa_2 & \chi & \kappa_1 + c_1 \kappa_2 & 0 & 0 & \dots & 0 \\ 0 & \kappa_1 - c_1 \kappa_2 & \chi & \kappa_1 + c_1 \kappa_2 & 0 & \dots & 0 \\ \vdots & \vdots & \vdots & \vdots & \vdots & \vdots & \vdots \\ 0 & \dots & 0 & 0 & \kappa_1 - c_1 \kappa_2 & \chi & \kappa_1 + c_1 \kappa_2 \\ 0 & \dots & 0 & 0 & 0 & \gamma_3 - c_1 \gamma_4 & \eta_3 - c_1 \eta_4 \end{bmatrix}$$

where the entries of the matrix depend on the discrete grid but not on the boundary conditions and where \mathbf{b} is determined by the boundary values. For

the numerical schemes in toy model 1,

$$\begin{aligned}
\eta_1 &= 1 - \frac{\Delta^2 + \Delta_1 \Delta}{\delta_1} \tau^2, & \eta_2 &= \frac{\Delta^2 - \Delta_1^2}{\delta_1} D, \\
\eta_3 &= 1 - \frac{\Delta^2 + \Delta_2 \Delta}{\delta_2} \tau^2, & \eta_4 &= \frac{\Delta^2 - \Delta_2^2}{\delta_2} D, \\
\gamma_1 &= \frac{\Delta_1 \Delta}{\delta_1} \tau^2, & \gamma_2 &= \frac{\Delta_1^2}{\delta_1} D, \\
\gamma_3 &= \frac{\Delta_2 \Delta}{\delta_2} \tau^2, & \gamma_4 &= \frac{\Delta_2^2}{\delta_2} D, \\
\kappa_1 &= \frac{1}{2} \tau^2, & \kappa_2 &= \frac{1}{2} D, \\
\chi &= 1 - \tau^2, & &
\end{aligned}$$

where

$$\begin{aligned}
\Delta t &= \tau \frac{\Delta}{c_1}, & D &= \frac{\Delta t}{\Delta}, \\
\Delta_1 &= (1 - \frac{1}{2}\epsilon)\Delta, & \Delta_2 &= \frac{N - \frac{1}{2}N\epsilon + \frac{1}{2}\epsilon^2}{N + \epsilon} \Delta, \\
\delta_1 &= \Delta_1^2 + \Delta_1 \Delta, & \delta_2 &= \Delta_2^2 + \Delta_2 \Delta.
\end{aligned}$$

Let us look for a constant solution to (A.3), $\mathbf{U} = \mathbf{U}^*$. For \mathbf{U}^* to be a solution, we must have

$$(M_1 - I)\mathbf{U}^* = \mathbf{b}, \quad (\text{A.4})$$

where I is identity matrix of order $N \times N$. In order to have a unique solution for (A.4), $\lambda = 1$ must not be an eigenvalue for M . Thus, the unique solution will be given by

$$\mathbf{U}^* = (M_1 - I)^{-1}\mathbf{b}.$$

Define now \mathbf{y}_n by

$$\mathbf{U}_n = \mathbf{y}_n + \mathbf{U}^*.$$

$$\begin{aligned}
\mathbf{y}_{n+1} + \mathbf{U}^* &= M_1(\mathbf{y}_n + \mathbf{U}^*) + \mathbf{b}, \\
\Downarrow \\
\mathbf{y}_{n+1} &= M_1\mathbf{y}_n.
\end{aligned} \quad (\text{A.5})$$

The matrix M_1 is not symmetric, but numerical investigations show that it in general has N different eigenvalues, $\lambda_i, i = 1, 2, \dots, N$. Then the corresponding eigenvectors, \mathbf{y}_i , are then independent and form a basis for \mathbb{R} . Let now $\mathbf{y}_0 \in \mathbb{R}$ be an initial value for (A.5). Then we have

$$\begin{aligned}
\mathbf{y}_0 &= \sum_i d_i \mathbf{y}_i, \\
\Downarrow \\
\mathbf{y}_n &= M_1^n \mathbf{y}_0 = \sum_i d_i \lambda_i^n \mathbf{y}_i.
\end{aligned}$$

We can see that if there exists any eigenvalue that is located outside the unit circle, then $\|\mathbf{y}_n\| \rightarrow \infty$. To obtain a stable numerical solution to model (A.1), the eigenvalues of M_1 must satisfy

$$\max_i |\lambda_i| < 1.$$

Using this result we find that the stability domain as a function of ϵ is of the form

$$\tau_1(\epsilon) \frac{\Delta x}{c_1} < \Delta t < \tau_2(\epsilon) \frac{\Delta x}{c_1}. \quad (\text{A.6})$$

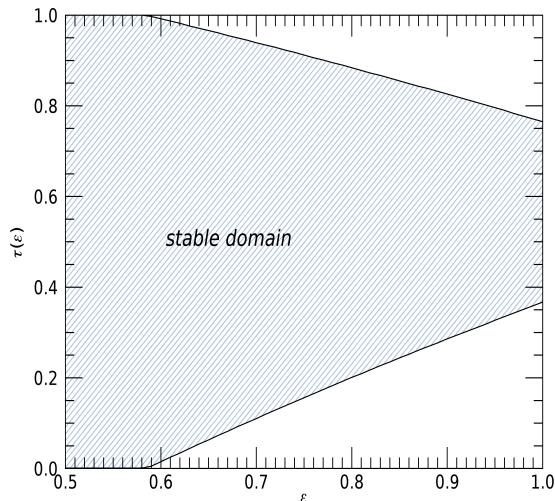


Figure A.1: The stability domain for the EOS formulation of (A.1).

It is evident from Fig A.1 that the restriction on the stability domain for the EOS formulation of (A.1), as compared to the Lax-Wendroff scheme for the case of free space propagation, is caused by the introduction of a nonuniform grid for the EOS formulation.

For model 2 we find the same stability domain as illustrated in Fig A.1 for model 1. That there should be some relation between the stability of these two models is perhaps not very surprising at the level of PDEs. After all, if we decouple the fields in model 2 from the current, the resulting system is equivalent to the wave equation and the solutions of that equation are sums of left and right going waves of the type described by Model 1. However, at the level of numerical schemes the coinciding of the stability domains for the two models is somewhat less obvious. Note that we can write the matrix M_1 , determining the stability for model 1, in the form

$$M_1 = m_1 + c m_1,$$

where m_1 and m_2 are $N \times N$ matrices given by,

$$m_1 = \begin{bmatrix} \eta_1 & \gamma_1 & 0 & 0 & 0 & \dots & 0 \\ \kappa_1 & \chi & \kappa_1 & 0 & 0 & \dots & 0 \\ 0 & \kappa_1 & \chi & \kappa_1 & 0 & \dots & 0 \\ \vdots & \vdots & \vdots & \vdots & \vdots & \vdots & \vdots \\ 0 & \dots & 0 & 0 & \kappa_1 & \chi & \kappa_1 \\ 0 & \dots & 0 & 0 & 0 & \gamma_3 & \eta_3 \end{bmatrix},$$

$$m_2 = \begin{bmatrix} \eta_2 & \gamma_2 & 0 & 0 & 0 & \dots & 0 \\ -\kappa_2 & 0 & \kappa_2 & 0 & 0 & \dots & 0 \\ 0 & -\kappa_2 & 0 & \kappa_2 & 0 & \dots & 0 \\ \vdots & \vdots & \vdots & \vdots & \vdots & \vdots & \vdots \\ 0 & \dots & 0 & 0 & -\kappa_2 & 0 & \kappa_2 \\ 0 & \dots & 0 & 0 & 0 & -\gamma_4 & -\eta_4 \end{bmatrix}.$$

Given this, the $2N \times 2N$ matrix determining the stability of model 2 is given by

$$M_2 = \begin{bmatrix} m_1 & \mu_1 m_2 \\ -\nu_1 m_2 & m_1 \end{bmatrix}.$$

The matrix M_2 clearly has a block structure and the same blocks give a linear decomposition of M_1 into a sum of two terms. However, we were not able use these commonalities between M_1 and M_2 to explain the fact that model 1 and model 2 have, not approximately, but exactly the same domain of stability as far as we can determine. Note that the occurrence of a stability domain like (A.6) might be a universal feature of EOS formulations. We have for example found a stability domain of this type in the EOS formulation of 3D Maxwell's equations. There, however, it is clear that the delay boundary conditions is at least partly responsible for the width of the stability domain.

References

- [1] K. Yee. Numerical solution of initial boundary value problems involving Maxwell's equations in isotropic media. *IEEE Transactions on Antennas and Propagation*. 1966 May, 14(3):302-307.
- [2] A. Taflove. Application of the finite-difference time-domain method to sinusoidal steady state electromagnetic penetration problems. *IEEE Transactions on Electromagnetic Compatibility*. 1980, 22(3): 191-202.
- [3] A. Taflove et. al. *Computational Electrodynamics: the Finite-Difference Time-Domain Method*, 3rd Ed. Artech House Publishers, 2005.
- [4] J. Berenger. A perfectly matched layer for the absorption of electromagnetic waves. *Journal of computational physics*. 1994, 114(2): 185-200.
- [5] S. Gedney. An anisotropic perfectly matched layer absorbing media for the truncation of FDTD lattices. *IEEE Transactions on Antennas and Propagation*. 1996, 44(12): 1630-1639.

- [6] W. C. Chew and W. H. Weedon. A 3d perfectly matched medium from modified Maxwell's equations with stretched coordinates. *Microwave and Optical Tech. Lett.* 1994, 7(13): 599-604.
- [7] Steven G. Johnson. Notes on Perfectly Matched Layers. Technical report, MIT, 2007.
- [8] D. N. Pattanayak and E. Wolf. General form and new interpretation of the Ewald-Oseen extinction theorem. *Optics communications.* 1972, 6(3): 217-220.
- [9] H. F. C. Brehm. Immersed interface method for solving the incompressible Navier-Stokes equations with moving boundaries. 49th AIAA Aerospace Science meeting Including the New Horizons Forum and Aerospace Science Exposition 2011.
- [10] Yong Zeng and Walter Hoyer and Jinjie Liu and Stephan W. Koch and Jerome V. Moloney. Classical theory for second-harmonic generation from metallic nanoparticles. *Physical Review B.* 2009, 79: 235109.
- [11] P. D. Lax and B. Wendroff. Systems of conservation laws. *Communications in pure and applied mathematics.* 1960, 13(2): 217-237.